

Radio Sources in Low-Luminosity Active Galactic Nuclei. I. VLA Detections of Compact, Flat-Spectrum Cores

Neil M. Nagar¹, Heino Falcke², Andrew S. Wilson^{1,3}, Luis C. Ho⁴

ABSTRACT

We report a high resolution ($0''.2$), 15 GHz survey of a sample of 48 low-luminosity active galactic nuclei with the Very Large Array¹. Compact radio emission has been detected above a flux density of 1.1 mJy in 57% (17 of 30) of low-ionization nuclear emission-line region (LINER) nuclei and low-luminosity Seyferts. The 2 cm radio power is significantly correlated with the emission-line ([O I] $\lambda 6300$) luminosity. Using radio fluxes at other frequencies from the literature, we find that at least 15 of the 18 detected radio cores have a flat to inverted spectrum ($\alpha \geq -0.3$, $S_\nu \propto \nu^\alpha$). While the present observations are consistent with the radio emission originating in star forming regions (the brightness temperatures are $\geq 10^{2.5-4.5}$ K), higher resolution radio observations of 10 of the detected sources, reported in a companion paper (Falcke et al. 2000), show that the cores are very compact (\lesssim pc), of high brightness temperature ($T_b \gtrsim 10^8$ K) and probably synchrotron self-absorbed, ruling out a starburst origin. Thus, our results suggest that at least 50% of low-luminosity Seyferts and LINERs in the sample are accretion powered, with the radio emission presumably coming from jets or advection-dominated accretion flows. We have detected only 1 of 18 “transition” (i.e. LINER + H II) nuclei observed, indicating their radio cores are significantly weaker than those of “pure” LINERs.

Compact 2 cm radio cores are found in both type 1 (i.e. with broad H α) and type 2 (without broad H α) nuclei. There is weak evidence, limited in significance by small numbers, that low-luminosity active galactic nuclei with compact radio cores exhibit radio ejecta preferentially aligned along the rotation axis of the galaxy disk. If this result is confirmed by a larger sample, it would lend support to the idea that the misalignment of accretion disks with the galaxy stellar disk in more luminous Seyfert galaxies is a result of radiation-pressure induced warping of their accretion disks.

¹Department of Astronomy, University of Maryland, College Park, MD 20742; neil@astro.umd.edu, wilson@astro.umd.edu

²Max-Planck-Institut für Radioastronomie, Auf dem Hügel 69, 53121 Bonn, Germany; hfalcke@mpifr-bonn.mpg.de

³Adjunct Astronomer, Space Telescope Science Institute

⁴Observatories of the Carnegie Institution of Washington, 813 Santa Barbara St., Pasadena, CA 91101; lho@ociw.edu

¹The VLA is operated by the National Radio Astronomy Observatory, a facility of the National Science Foundation operated under cooperative agreement by Associated Universities, Inc.

Subject headings: accretion, accretion disks — galaxies: active — galaxies: Seyfert — galaxies: nuclei — radio continuum: galaxies — surveys

1. Introduction

There is increasing evidence that a large fraction of the nuclei of nearby galaxies show many similarities with powerful active galactic nuclei (AGN); these objects are termed low-luminosity active galactic nuclei (LLAGN; active galaxies with nuclear $L_{H\alpha} \leq 10^{40}$ erg s⁻¹; Ho, Filippenko & Sargent 1997a, hereafter H97a). These similarities include broad H α lines (Ho et al. 1997b), broader H α lines in polarized emission than in total emission (Barth et al. 1999), nuclear UV sources (Maoz et al. 1995; Barth et al. 1998) and water vapor megamasers (Braatz et al. 1997). However, the emission-line spectra of LLAGNs (i.e. low-luminosity Seyferts, LINERs, and “transition” nuclei [nuclei with spectra intermediate between those of LINERs and H II regions]), can also be modeled in terms of photoionization by hot, young stars (Terlevich & Melnick 1985; Filippenko & Terlevich 1992; Shields 1992), by collisional ionization in shocks (Koski & Osterbrock 1976; Fosbury et al. 1978; Heckman 1980; Terlevich et al. 1992; Dopita & Sutherland 1995), or by aging starbursts (Alonso-Herrero et al. 1999). Thus, it is not clear that accretion onto a black hole powers all LLAGNs.

How does one distinguish accretion-powered LLAGNs from LLAGNs powered by hot stars or supernova shocks? Broad H α lines and bright unresolved optical or UV sources are ambiguous indicators because they can all be produced in starburst models (see Terlevich et al. 1992), and a search for broader polarized H α emission is currently feasible in only a few of the brightest LLAGNs (Barth et al. 1999). Further, all these indicators are highly dependent on viewing geometry and obscuration and on the signal to noise of the observations, a problem exacerbated by the low optical and UV luminosities of LLAGNs. Their observation demands both high signal-to-noise spectra and high spatial resolution to separate weak nuclear emission lines from the starlight of the host galaxy.

One well-known property of some powerful AGNs is a compact, flat-spectrum nuclear radio source, usually interpreted as the synchrotron self-absorbed base of the jet which fuels larger-scale radio emission. Astrophysical jets are known to be produced in systems undergoing accretion onto a compact object (e.g. Pringle 1993; Blandford 1993), so such compact radio sources in galactic nuclei may reasonably be considered a signature of an AGN. Much theoretical work (e.g. Begelman, Blandford & Rees 1984; Lovelace & Romanova 1996; Falcke & Biermann 1999) has been devoted to this disk-jet relationship in the case of galactic nuclei and it has been suggested that scaled-down versions of AGN jets can produce flat-spectrum radio cores in LLAGNs (Falcke 1996; Falcke & Biermann 1996). Nuclear radio emission with an inverted spectrum is also expected from an advection-dominated accretion flow (ADAF; e.g. Narayan et al. 1998), a possible form of accretion onto a black hole at low accretion rates (Rees et al. 1982), or from bremsstrahlung, cyclotron and synchrotron emission from plasma accreting quasi-spherically onto a black hole (Melia 1994). From the observational perspective, Heckman (1980) showed that LINER nuclei tend to be associated

with a compact radio source, and compact, flat-spectrum radio cores are known to be present in many ‘normal’ E/S0 galaxies (Sadler et al. 1989; Wrobel & Heeschen 1991; Slee et al. 1994). Flat-spectrum radio cores are, however, uncommon in normal spirals or Seyfert galaxies (Ulvestad & Wilson 1989; Vila et al. 1990; Sadler et al. 1995). Flat-spectrum radio sources can also result through thermal emission from optically-thin ionized gas or through free-free absorption of non-thermal radio emission, a process which probably occurs in compact nuclear starbursts (Condon et al. 1991). The brightness temperature, T_b , in such starbursts is limited to $\log [T_b \text{ (K)}] \lesssim 5$ (Condon et al. 1991). Thus it is necessary to show that T_b exceeds this limit before accretion onto a black hole can be claimed as the power source.

In this paper, we present a high-frequency (15 GHz or 2 cm), high-resolution ($\sim 0''.15$) survey of LLAGNs with the Very Large Array (VLA, Thompson et al. 1980). This resolution is high enough to isolate nuclear emission from that of the host galaxy, and the radiation is unaffected by the obscuration present at UV or optical wavelengths, and less affected by free-free absorption than observations at longer cm wavelengths. Further, large samples can be quickly studied, as deep radio maps are achievable in as little as 15–20 min per object. Higher resolution follow-up observations are then required in order to eliminate the possibility that the radio cores are thermal in origin, as discussed above. We have therefore embarked on a program to observe a large number of LLAGNs at high resolution with the VLA and the Very Long Baseline Array (VLBA, Napier et al. 1994) in order to identify accretion-powered nuclei, to test the predictions of ADAF and jet models, and to characterize the presence and structure of radio jets on sub-pc to hundred-pc scales. In this paper, we report on the results of the first stage of this program — VLA observations of 48 LLAGNs which have been extensively observed at other wavebands. Preliminary results of this project have been published in Falcke et al. (1997, 1998, 1999) and Nagar et al. (1999b).

2. Sample, Observations and Data Reduction

A total of 48 galaxies were selected from the magnitude-limited Palomar spectroscopic survey of 486 nearby bright galaxies (Ho, Filippenko, & Sargent 1995). All 48 galaxies were originally selected, using preliminary spectral classification, to have nuclei with “pure” LINER or “transition object” (composite LINER + H II) characteristics. The spectral type of 8 of the nuclei was somewhat uncertain, and these galaxies were later reclassified as Seyferts (H97a). Thus, our sample of 48 LLAGNs consists of 22 “pure” LINERs, 18 “transition objects,” and 8 low-luminosity Seyferts. The 48 objects were not selected by well-defined criteria; they were individually chosen for study at multiple wavelengths because they were particularly “interesting” LLAGNs. Our sample is the subject of a rigorous observational campaign involving radio observations at 2 cm (reported here), 3.6 cm and 6 cm (Ho et al. 2000), *Hubble Space Telescope* (*HST*) optical (Peng et al. 1998) and UV imaging (Maoz et al. 1995; Barth et al. 1998) as well as spectroscopy (Maoz et al. 1998), and X-ray imaging by the *Chandra* observatory.

All 48 LLAGNs in the sample, plus two additional objects – NGC 4449 (whose nuclear spectrum

is that of an H II region) and NGC 5756 (a southern spiral not in the Palomar spectroscopic survey) – were observed by the VLA over three runs on 1996 October 7, 11 and 18, while the array configuration was being changed from ‘D’ to ‘A’ (see Thompson et al. 1980 for a description of the VLA configurations). The weather was fair for all runs with clear skies and temperatures between 0 and 23°C. Two 8 min observations of each galaxy were sandwiched between three 2 min observations of a nearby phase calibrator, so that the total time on source was typically 16 min. For the October 7 run, there were 9 antennas at A-configuration pads plus 18 antennas at D-configuration pads. Five D-configuration antennas were taken out of the array at various times during the run to be moved to their A-configuration pads; they did not start observing again until after our run was completed. A sixth D-configuration antenna was removed from the array for painting. Of the nine antennas at A-configuration pads, the data from the three most recently moved were unusable, since the antenna positions were poorly determined. For the October 11 run, 25 of the 27 antennas were on their A-configuration pads, but the data from the four most recently moved antennas were unusable as their positions were poorly determined. For the October 18 run, all except one of the antennas were at their A-configuration pads, and all had reasonably well-determined positions.

The data were calibrated using the AIPS software, following the standard procedures outlined in the AIPS cookbook. Since positions for recently-moved antennas were not well determined at the time of observations, antenna positions listed in the data files were updated with the corrections to the positions found by VLA operators over the few weeks after the observations. We found that using all position corrections up to those determined on November 23, 1996, led to the best calibrator phase solutions for most of the recently-moved antennas. Other bad data were removed before the phase solutions, derived from the phase calibrators, were applied to the target galaxies. On the October 7 and October 18 runs, the source 1328+307 (3C 286) was observed twice and used to set the flux-density scale to that of Baars et al. (1977). On the shorter October 11 run, an observation of 0404+768 was used to set the flux-density scale (we used a 2 cm flux-density of 1.46 Jy for this source). The phase calibrator flux-densities were bootstrapped to that of 0404+768, and the bootstrapped values were found to be in good agreement with those listed in the VLA flux-density database (part of the “VLA calibrator manual”; available on-line at <http://www.nrao.edu>).

The maps were made with AIPS task IMAGR. For the October 7 run, we imaged each object twice, once using only the antennas on D-configuration pads, which resulted in $\sim 5''$ -resolution maps, and once using only those baselines which included at least one antenna on an A-configuration pad, which resulted in $\sim 0''.15$ resolution maps. For the other two runs, a single map was made for each source, using all antennas. For sources stronger than about 3 mJy, we were able to iteratively self-calibrate the data so as to increase the signal-to-noise ratio in the final map. Phase-only self-calibration was found to give good results, with little further improvement from a combined amplitude & phase self-calibration. The typical r.m.s. noise in the maps prior to self-calibration was 0.1 mJy. Many of the maps of the undetected nuclei show 4 to 5 σ peaks at various locations in the map. We therefore conservatively use 10 times the r.m.s. noise in the map as the upper limit

for the flux density of the undetected sources, so the sensitivity of our survey is about 1.1 mJy.

On the October 11 run, NGC 266, NGC 404, and NGC 7217 were also observed at 0.7 cm and 3.6 cm, with the VLA split into two subarrays which observed at different frequencies (not all antennas had 0.7 cm receivers). These data were reduced as described above. An observation of 0404+768 was used to set the flux-density scale at 0.7 cm. We set the 0.7 cm flux density of 0404+768 to 578.2 mJy for the AC IF’s and 575.3 for the BD IF’s, after finding, from the VLA flux-density database, that these were the flux densities on 1997 February 24, the date closest to our run that the source was observed (the flux density stayed between 500 and 600 mJy for the following ~ 300 days). The flux density of the phase calibrators, 0055+300 and 2201+315, were bootstrapped to that of 0404+768, and the results were consistent with the values listed in the flux-density database. At 3.6 cm, the observation of 3C 48 could not be used to set the flux-density scale, as the four innermost antennas (and almost every alternate antenna on each arm) were observing at 0.7 cm, so that none of the 3.6 cm interferometer baselines was small enough for an accurate flux-density calibration solution (the VLA calibrator manual specifies that A-configuration observations of this calibrator should be restricted to 0–40 k λ). We therefore set the flux density of 2201+315 (the phase calibrator for NGC 7217) to 2.51 Jy in both AC and BD IF’s at 3.6 cm, as this was its measured value on 1997 January 17, the date closest to our run (after this date, the flux density of this source rose steadily to 3.5 Jy over the next ~ 300 days and then stayed roughly constant). The flux density of 0055+300 (the phase calibrator for NGC 266 and NGC 404) was then bootstrapped from that of 2201+315. The result, $S(0055+300) = 0.82$ Jy, is consistent with the values listed in the flux-density database for this source. Nevertheless, the 3.6 cm and 0.7 cm flux densities of the three galaxies are subject to additional uncertainty.

All data were calibrated and imaged independently by two of us (NMN and HF), yielding consistent results (all corrections for antenna positions were also independently done). We are therefore confident of the results, despite the uncertainties caused by the uncertain antenna positions.

3. Results

3.1. Detection Rate

The results of the VLA observations are listed in Table 1, with columns explained in the footnotes. The radio positions for the 22 detected objects are limited by the positional accuracy of the phase calibrators, which is typically 2–10 milli-arcsec (mas), and by the accuracy of the Gaussian fit to the source brightness distribution, which depends on the signal to noise ratio of the source detection. The overall accuracy should typically be better than ~ 50 mas for all target sources detected in A-configuration, and better than 500 mas for target sources detected in only D-configuration. We have compared the radio positions derived here with optical positions from Cotton, Condon, & Arbizzani (1999), which were measured from the digital sky survey with typical 1σ accuracy $1''.5$ – $2''.5$ in each of right ascension and declination. For all but two of the 2 cm

detected nuclei, the radio and optical positions agree to within $1''$ – $3''.5$ (see Table 1). In NGC 185 and NGC 4550, the offsets between radio and optical positions are significant, and as discussed in Appendix A, it is possible that the radio sources we detected in these two galaxies are not related to the galaxy nucleus.

Assuming that the radio sources towards NGC 185 and NGC 4550 are in fact associated with their nuclei, the detection rate of 2 cm radio cores in the A-configuration maps of our LLAGN sample is 37% (18 of 48), at a 10σ detection limit of 1.1 mJy. The rate is more striking if we consider the detection rates for low-luminosity Seyferts (75%; 6 of 8) and for LINERs (50%; 11 of 22). On the other hand, only one of the 18 observed ‘transition’ nuclei was detected. The morphological type of the galaxy with the detected transition nucleus, NGC 5866, is one of the earliest of the transition objects observed. An additional four objects were detected in D- but not A-configuration maps; we do not consider these four as nuclei with compact 2 cm radio cores. In comparison, Wrobel & Heeschen (1991) detected 30% (64 of 210) of all E/S0 galaxies with $D < 40$ Mpc and $m_B < 14$ mag in a 6 cm VLA survey with resolution $5''$ and 10σ detection limit 1 mJy; the lower resolution and lower frequency make their survey more prone to detecting emission from sources unrelated to the central engine.

The radio luminosities of most of the detected 2 cm cores are between $10^{19.3}$ and 10^{22} W Hz^{-1} (Fig. 1), similar to the luminosities seen in ‘normal’ E/S0 galaxies (Sadler et al. 1989). It is notable, however, that a significant fraction of the detected 2 cm compact cores are in spiral galaxies (Fig. 1).

The 0.7 cm maps of NGC 404, NGC 266, and NGC 7217 were, as expected, noisy, and all three galaxies were undetected at a 10σ limit of 10 mJy. At 3.6 cm, NGC 266 and NGC 7217 were detected as unresolved sources with flux densities 3.1 mJy and 1.2 mJy, respectively, while NGC 404 was not detected at a 10σ upper limit of 0.9 mJy.

3.2. Compact, Flat-Spectrum Cores

None of the objects show reliable extended structure in either A- or D-configuration maps. This is not surprising as the high resolution may resolve out most extended emission, which is expected to be weak at the high frequency observed. For a few sources, a Gaussian fit (with peak flux-density, major and minor axes as free parameters) to the nuclear radio source brightness distribution results in a Gaussian size slightly larger than the beam size so that the peak flux-density is slightly smaller than the total flux-density (see Table 1); however, the deconvolved source sizes are much smaller than half the beam size, so we consider these sources as unresolved. Of the 8 objects which are detected in both our A- and D-configuration maps, NGC 2655 is the only one with significantly more flux density at $5''$ resolution than at $0''.15$ resolution. Thus, most of the detected 2 cm nuclear radio sources are compact at the $0''.15$ resolution (typically 15–25 pc) of our survey. The implied brightness temperatures for the 2 cm compact nuclei are $T_b \geq 10^{3.0-4.0}$ K except for NGC 4278

and NGC 6500 which have $T_b \geq 10^{4.5}$ K, and NGC 185, NGC 4548, NGC 4550, NGC 4636 and NGC 5033 which have $T_b \geq 10^{2.5-3.0}$ K.

We have supplemented our 2 cm observations with radio data at other wavelengths from the literature, such as the 6 cm radio survey of Wrobel & Heeschen (1991) and the 20 cm VLA FIRST survey catalog (White et al. 1997, hereafter FIRST), in order to derive non-simultaneous spectral indices for the 2 cm detected nuclei; details of the spectral index determination are listed in Appendix A for each galaxy detected at 2 cm. While the actual value of the spectral index is uncertain, given the resolution mismatch and the non-simultaneity of the observations, we can determine whether the core is flat spectrum ($\alpha \geq -0.3$; $S_\nu \propto \nu^\alpha$), or steep spectrum ($\alpha < -0.3$), as noted in column 13 of Table 1. Since compact flat-spectrum radio sources are often variable, the use of non-simultaneous data at two frequencies can cause some intrinsically flat-spectrum radio sources to be misclassified as steep-spectrum sources. However, since extended steep-spectrum radio sources are not variable, the use of non-simultaneous data at two frequencies should rarely cause intrinsically steep-spectrum radio sources to be misclassified as flat-spectrum sources. Also, since the resolution is better at the higher frequency, resolution effects will tend to steepen the measured spectrum if extended emission is present. Thus we are confident of the reality of the flat spectra obtained.

Fifteen of the 18 objects detected in our A-configuration 2 cm maps show a flat-spectrum radio core, and one has an undetermined radio spectrum. The remaining two objects detected in the A-configuration 2 cm maps, NGC 2655 and NGC 4636, show evidence for the presence of a steep-spectrum radio core, although NGC 4636 has “jet”-like steep-spectrum nuclear radio extensions (Stanger & Warwick 1986) which may dominate over any flat-spectrum nuclear component within the beam of the radio maps. In the case of NGC 2655, the inferred steep-spectrum of the nucleus is consistent with the presence of extended 2 cm radio emission.

The radio morphology of the LLAGNs detected at 2 cm is different from what is seen in “classical” Seyferts (Ulvestad & Wilson 1989; Nagar et al. 1999a), where the nuclear radio emission is usually dominated by steep-spectrum “jet” or double radio components on tens to hundreds of pc scales, and any pc-scale radio core may potentially be hidden by free-free absorption at cm wavelengths (e.g., Ulvestad et al. 1981; Gallimore et al. 1999). The high incidence of compact, flat-spectrum radio cores in the spiral galaxies in our sample is unusual (e.g., Vila et al. 1990; Sadler et al. 1995). In fact, the high incidence of flat-spectrum radio cores in low-luminosity Seyferts is also unusual, given that flat-spectrum compact radio cores are found in only about 10% of “classical” Seyferts (de Bruyn & Wilson 1978; Ulvestad & Wilson 1989; Sadler et al. 1995).

3.3. The Relationship Between Radio and Emission-line Luminosities

Correlations between the emission-line and radio luminosities of active galaxies are well known, and are found in both Seyfert (de Bruyn & Wilson 1978) and radio galaxies (Baum & Heckman

1989). The [O III] $\lambda 5007$ line is usually used in assessing these correlations, but this line is weak in LINERs and we use instead [O I] $\lambda 6300$, which also has the advantage of being uncontaminated by emission from H II regions. In our LLAGN sample, the 2 cm radio power appears closely correlated with the nuclear [O I] $\lambda 6300$ luminosity (Fig. 2a and 2b). Testing the statistical significance of this apparent correlation is not straightforward as there exist both upper limits (line not detected) and highly uncertain values (non-photometric data) for the [O I] $\lambda 6300$ luminosities, along with upper limits to the 2 cm radio powers. Eight of the LLAGNs in the sample have non-photometric [O I] $\lambda 6300$ flux densities. We treated these eight flux densities as photometric measurements when using the bivariate tests from the ASURV statistical software package (Lavalley et al. 1992, hereafter ASURV). This approximation should not bias the results significantly as the uncertainties in the flux density are expected to be much less than an order of magnitude. When this is done, tests on the whole sample indicate a correlation between the radio and [O I] $\lambda 6300$ luminosities at the 97% significance level. Deleting NGC 185 (the point at the bottom left corner of Fig. 2a), for which the association of the radio source with the nucleus is uncertain (Section 3.1), lowers the significance level by only 1%.

3.4. The 2 cm Non-detections

Do the LLAGNs undetected at 2 cm truly lack radio cores, or do a significant fraction of them have radio cores which are weaker than those in the detected LLAGNs because of, for example, a lower bulge luminosity (Sadler et al. 1989) or a later morphological type? The distributions of host galaxy bulge luminosity and distance (as listed in H97a) are more or less similar for the detected and undetected LINERs. The 2 cm compact core LINERs have a median host galaxy morphological type ($T_{median} = -1.5$) which is earlier than, and a median [O I] $\lambda 6300$ luminosity ($\text{Log } L_{[\text{O I}]}(\text{median}) = 31.5$ Watts) which is higher than, that for LINERs without compact 2 cm cores ($T_{median} = 2.0$, $\text{Log } L_{[\text{O I}]}(\text{median}) = 31.1$ Watts), though the difference is not statistically significant. Given the correlation between emission-line and radio luminosity, it is possible that deeper radio imaging will find compact radio cores in the 2 cm undetected LINERs. The host galaxies of the two undetected Seyferts have bulge luminosities in the B band among the lowest of the eight Seyferts in our sample. There is no clear difference between the morphological types of the detected and undetected Seyferts.

Seventeen of the non-detected nuclei are “transition objects.” Statistical tests from the ASURV package indicate that the distributions of the 2 cm radio power of LINERs and transition objects in the sample are different at a confidence level of 99.3–99.5%. While the numerical value of the significance level is questionable given that there is only one detection among the transition objects, arbitrarily changing the four transition objects with the lowest radio flux-density upper limits into radio detections still results in a difference between transition object and LINER radio powers at the 92–98% significance level. While the transition nuclei have somewhat lower median bulge luminosities and generally later morphological types compared to the detected LINERs, the

statistical significance of these differences is not high. Not unexpectedly, the transition objects in our sample do appear to have weaker [O I] λ 6300 luminosities as compared to the LINERs and Seyferts (Fig. 2). If the non-photometric [O I] λ 6300 flux measurements are considered to be accurate, statistical tests from the ASURV package indicate that in our sample the [O I] λ 6300 luminosities of the transition objects are lower than that of LINERs and Seyferts at the $\sim 99.8\%$ significance level. It remains to be seen whether this luminosity difference is large enough to explain the striking difference in the detection rates. Surprisingly, the one transition nucleus detected at 2 cm, NGC 5866 (the rightmost circle in Fig. 2b), has one of the lowest [O I] λ 6300 luminosities among the transition nuclei.

3.5. Other AGN indicators

We find compact 2 cm radio cores in both type 1 and type 2 nuclei, that is, those with and without visible broad H α emission. Furthermore, some type 1 nuclei in our sample (two Seyferts and four LINERs) do not have a compact radio core at our detection limits. Among LINERs, 64% (7 of 11) of type 1 nuclei host compact radio cores, as compared to only 36% (4 of 11) of type 2 nuclei.

Additional evidence supports the accretion-powered nature of the nuclei with compact, flat-spectrum 2 cm cores. NGC 4579 is one of the very few LLAGNs with a detected Fe K α line (Terashima et al. 1998, 2000); such lines are believed to originate through fluorescence in an accretion disk. The optical–UV spectrum of NGC 4579 has been studied in detail by Barth et al. (1996), who show that the broad-line region in this object is detectable in a number of permitted transitions. The broad-band spectral energy distribution of NGC 4579 (Ho 1999) has been interpreted in the context of an ADAF model (Quataert et al. 1999). NGC 4278 and NGC 6500 are both known to harbor pc-scale radio cores studied with Very Long Baseline Interferometry (VLBI) techniques (Jones 1984; Jones et al. 1981; Falcke et al. 2000), and NGC 4203 (Shields et al. 2000), NGC 4278 and NGC 4636 (Magorrian et al. 1998) show kinematic evidence for massive dark objects at their centers. Maoz et al. (1998) find that the nuclei of NGC 404, NGC 4569, and NGC 5055, all undetected at 2 cm, contain massive stars which probably generate sufficient ionizing photons to power the optical emission lines, so it is not necessary to invoke an accretion-powered source. On the other hand, they find that the nuclei of M 81, NGC 4594, and NGC 6500 (and perhaps NGC 4579) exhibit a severe “deficit” in ionizing photons (i.e. apparently insufficient photons shortward of the Lyman limit, as inferred through extrapolation of the observed UV spectrum, to power the optical and UV emission lines), but their X-ray/UV ratios are two orders of magnitude higher than those of the three stellar-powered LINERs. Maoz et al. (1998) concluded that, in these four objects a component that emits primarily in the extreme-UV may be the main photoionizing source. We observed and strongly detected two of these nuclei (NGC 4579 and NGC 6500) at 2 cm, and the other two are known to have pc-scale radio cores (Bartel et al. 1982; Graham et al. 1981). Finally, the lack of clear evidence for X-ray emission from an AGN in NGC 404, NGC 4111, NGC 4192,

and NGC 4569 (Terashima et al. 1999), galaxies undetected at 2 cm, is consistent with an absence of an accretion-powered source.

3.6. Minor-axis Jets or Outflows

A significant number of the LLAGNs with 2 cm compact radio cores in our sample show extended 20 cm radio emission in 5'' resolution FIRST maps, and/or 1''.5–4'' maps from other sources (see Appendix A). We therefore compared the P.A. of this radio extension, when available, with that of the host galaxy major axis for all LLAGNs in our sample which host 2 cm compact radio cores. The relevant P.A.'s are listed in Table 2, and a histogram of the difference in the two P.A.'s, δ , is shown in Fig. 3. The single transition object (shown in grey) shows extended emission along the host galaxy major axis, so it is likely that the radio emission is from the galaxy disk. On the other hand, LINERs and low-luminosity Seyferts with compact 2 cm radio cores appear to favor extended radio emission along the galaxy disk minor axis, although the small number of objects prohibits any meaningful statistical tests. The extent of this minor-axis radio emission is typically only 0''.5 to 3'' (50–350 pc for most galaxies in the sample), and could trace the inner parts of wide-angle, minor-axis outflows, as seen in classical Seyferts (Colbert et al. 1996), or low-luminosity collimated “jets” from the central engine.

4. Discussion

We have detected unresolved 2 cm nuclear radio emission in 75% of low-luminosity Seyferts and 50% of LINERs. At least 83% of these nuclear radio sources have flat radio spectra. At this point it is not clear whether the 2 cm non-detected LINERs and low-luminosity Seyferts really do not have compact radio cores, or whether their compact cores simply have lower radio luminosities or are hidden by, for example, free-free absorption. In powerful AGNs, compact flat-spectrum nuclear radio cores are widely accepted as the signature of synchrotron emission from the base of a synchrotron self-absorbed jet (see the review by Zensus 1997). The compact, flat-spectrum radio cores we detect in LLAGNs could be scaled-down versions of powerful AGNs (e.g. Falcke et al. 1999), or could trace emission from an ADAF (Narayan et al. 1998), or material undergoing quasi-spherical accretion (Melia 1992). Alternatively, the radio cores could be produced by thermal bremsstrahlung from ionized gas or by synchrotron radiation which has suffered free-free absorption. Such emission could originate from an active nucleus or nuclear star forming regions. The lower limits to the brightness temperatures, T_b^{2cm} , of the 2 cm compact core objects in our sample are $10^{2.5-4.5}$ K, so the VLA observations alone cannot rule out the notion that the radio emission originates in star formation regions. However, most objects have brightness temperatures too high to be optically-thin thermal emission from a gas at 10^4 K. The expected value of T_b is $\sim 10^4$ K $(\nu/\nu_\tau)^{-2.1}$, where ν is the observing frequency and ν_τ is the frequency at which the source becomes optically thick. Many of our objects have a flat spectrum between 2 cm and 20 cm suggesting $\nu_\tau <$

1.4 GHz (20 cm). If this is the case, then thermal emission must have $T_b^{2cm} < 10^4(20/2)^{-2.1}$ K i.e. < 90 K, lower than all of our measurements. Further, higher resolution observations of 10 of the detected objects in this sample reveal brightness temperatures $\gtrsim 10^8$ K, strongly suggesting that synchrotron self-absorption is responsible for the flat spectra and arguing against a thermal origin (Falcke et al. 2000). Thus, it is very likely that at least 50% of the LINERs and low-luminosity Seyferts in our sample contain accretion-powered nuclei. Several independent factors, described in Section 3.5, support our proposition that the presence of a compact, flat-spectrum (as determined from VLA observations) radio core is related to the presence of accretion onto a massive black hole in LLAGNs.

The detection rate of radio cores in transition objects in our sample is dramatically low (1 of 18). The significant difference between transition and “pure” LINER detection rates, combined with the lack of any significant difference between their host galaxy properties, suggests one of the following. 1) The central engines of transition objects are intrinsically different from those of “pure” LINERs, or 2) Transition objects are truly composite nuclei with a LINER and an H II component (e.g. Ho et al. 1993), in which case both the LINER component and its radio emission are much weaker in transition objects than in “pure” LINERs. Using the luminosity in the [O I] $\lambda 6300$ line as an indicator of the luminosity of the LINER component, this second premise is supported by the results that the [O I] $\lambda 6300$ and 2 cm luminosities are correlated at the $\sim 97\%$ significance level, and that the [O I] $\lambda 6300$ luminosity of the transition objects is lower than that of the LINERs and Seyferts in the sample at the $\sim 99.8\%$ significance level (Fig. 2).

Finally, if the extended 20 cm radio emission, which appears preferentially aligned with the host galaxy minor axis in a subset of 2 cm compact core LLAGNs (Fig. 3), does trace jets from the central engine, there are interesting implications for the orientation of the central engines of AGN. Similar analyses of “classical” Seyferts (Ulvestad & Wilson 1984; Schmitt et al. 1997; Clarke et al. 1998; Nagar & Wilson 1999) have shown that the distribution of $P.A._{radio} - P.A._{galaxy\ major\ axis}$ is more or less uniform between 0° and 90° . One explanation for this uniform distribution is that radiation from the central engine illuminates the inner accretion disk inducing a “radiative instability” (Pringle 1997) which causes large warps in the inner disk. In this case, even if the outer accretion disk shares the same axis of rotation as the host galaxy disk, the jet (presumably launched along the axis of the inner accretion disk) may then be at a random angle with respect to the axis of the galaxy disk. If the radiation instability is indeed the correct explanation, then in LLAGNs, where the radiation field of the central engine is much weaker, the disk is expected to be less prone to the radiation instability (see e.g. equation 3.2 and Section 3.2 of Pringle 1997), so that the jet axis is more likely to be along the host galaxy rotation axis. This is precisely what we find. Alternately, the jet power in LLAGNs may be low enough that buoyancy dominates jet motions on the scale (typically 50–350 pc) of the extended emission, redirecting the jet along the minor axis. Our further surveys for 2 cm radio cores in LLAGNs and our completed observations of 17 nearby bright LLAGNs at $0''.3$ resolution with the Multi-Element Radio Linked Interferometer Network (MERLIN) at 20 cm will potentially reveal more on this subject.

5. Conclusions

Our detection of compact, flat-spectrum radio cores in about 50% of low-luminosity Seyferts and LINERs in a sample of 48 low-luminosity AGNs, when combined with VLBA observations (Falcke et al. 2000), suggests that at least half of all low-luminosity Seyferts and LINERs are accretion powered. Given the sensitivity limit of our survey, the true incidence of radio cores is likely to be higher. The 2 cm radio power is significantly correlated with the [O I] λ 6300 luminosity for LLAGNs in our sample. The lower detection rate (at $\geq 92\%$ significance) of compact radio cores in “transition” nuclei suggests that either these nuclei are intrinsically different from “pure” LINERs, or their “pure” LINER component is of lower luminosity, with correspondingly lower luminosity radio cores. The latter interpretation is favored by the correlation between the radio and [O I] λ 6300 luminosities coupled with the lower [O I] λ 6300 luminosities of the “transition” nuclei as compared to the LINERs.

The presence or absence of a detected broad $H\alpha$ line is not a good indicator of the presence or absence of a compact, flat-spectrum 2 cm radio core. A significant number of the LINERs and low-luminosity Seyferts which contain 2 cm compact radio cores show evidence, at low resolution ($1''$ – $5''$) and frequency (1.4 GHz or 20 cm), for extended radio emission along the galaxy disk minor axis. This radio emission may trace a wide-angle outflow or a weak, highly-collimated jet along the disk rotation axis. If the latter is true, it lends support to the idea that it is the “radiative instability” which causes warps in the nuclear accretion disks of more luminous Seyfert galaxies.

Finally, we note that the data presented here are the initial results of a larger program to study a well-defined sample of LLAGNs at high resolution with the VLA and VLBA; results of these will appear in future papers in this series.

This research has been supported by NSF grant AST 9527289 and by NASA grant NAG 81027. The work of HF is funded by DFG grant Fa 358/1-1 & 2. The work of L. C. H. is partly funded by NASA grant NAG 5-3556, and by NASA grants GO-06837.01-95A and AR-07527.02-96A from the Space Telescope Science Institute (operated by AURA, Inc., under NASA contract NAS5-26555).

A. Notes on Individual Objects

Specific notes on all galaxies detected at 2 cm and on some undetected galaxies are listed here.

NGC 185 The 2 cm source we detect is offset $14''.5$ west and $4''$ north of the optical position determined by Cotton et al. (1999) from digital sky survey plates. The 1σ error of the optical position determination is estimated to be $2''.7$ in each of right ascension and declination. The galaxy is diffuse, $\sim 12' \times 10'$ in extent, and has a prominent dust lane to the north-west which may bias the optical position determination. Overlaying the optical and radio images shows that the

2 cm radio source lies at the south-west tip of the dust lane, and the offset from the optical center does appear to be more than can be explained by dust lane obscuration. Further, the radio source has a very low luminosity ($10^{16.7}$ Watts Hz^{-1}) which can be explained by a source in the galaxy stellar disk. Hummel (1980) lists a 5σ upper limit of 10 mJy in a $23''$ resolution map at 20 cm, and we find a 2 cm flux density of 0.8 mJy in our $0''.15$ map. It is therefore possible that the source is flat spectrum, but a measurement at a resolution closer to that of the 2 cm map is required for a definitive result, and for now we consider this source to have an undetermined spectral index.

NGC 266 Our simultaneous 3.6 cm and 2 cm observations on 1996 October 11, with resolutions $0''.29 \times 0''.24$, and $0''.15 \times 0''.13$, detected an unresolved nuclear source with flux densities 3.1 mJy and 4.1 mJy, respectively. The nucleus therefore has an inverted radio spectrum, $\alpha_2^{3.6} \geq 0.5$. This source was, however, not detected at a 10σ upper limit of 10 mJy in our simultaneous 0.7 cm observation. NGC 266 has been identified with source NVSS J004947+321637 by the NASA Extragalactic Database (NED; Helou et al. 1991) i.e. it has been detected in the 20 cm NRAO VLA sky survey (NVSS), with a peak flux-density of 8.9 mJy/beam at a resolution of $45''$, though the 20 cm position is offset $44''$ from our 2 cm position. In any case, 8.9 mJy may be taken as an upper limit to the 20 cm flux density.

NGC 404 Our simultaneous 3.6 cm, 2 cm, and 0.7 cm observations on 1996 October 11 did not detect the nucleus at 10σ upper limits of 0.9 mJy, 1.3 mJy, and 10 mJy, respectively.

NGC 2655 Comprehensive radio continuum and optical emission-line imaging, as well as optical spectra, are presented by Keel & Hummel (1988). Their VLA 6 cm map shows a roughly E-W symmetric extension at $0''.5$ resolution (with a peak flux-density of 36 mJy/beam from a component with half-power size $0''.4 \times 0''.5$). Combining this peak flux-density with our 2 cm peak flux-densities of 6 mJy/beam and 13.4 mJy/beam at resolutions of $0''.15$ and $5''$, respectively, results in a non-simultaneous spectral index, $\alpha_2^6 = -0.7$ to -1.6 , for the radio emission within $0''.5$ of the nucleus. Keel & Hummel (1988) find $S_\nu \propto \nu^{-0.67}$ for the nucleus, from $4''$ resolution non-simultaneous VLA maps at 6 and 20 cm. They also find a secondary 6 cm source in P.A. 117° , with a diffuse bridge of radio emission joining it to the nuclear component. The morphology, kinematics, and line ratios of the surrounding emission-line gas, suggest that this secondary 6 cm source and bridge are related to nuclear ejecta (Keel & Hummel 1988). Clearly, most of the radio emission in this object is extended, and if the emission from the unresolved radio nucleus is related to an accreting black hole, then its steep radio spectrum suggests that it is more likely that the emission is from synchrotron-emitting jets, rather than from a compact radio core. The host galaxy P.A. is not defined for this galaxy in the Uppsala General Catalogue of Galaxies (Nilson 1973, hereafter UGC) or the Third Reference Catalogue of Bright Galaxies (de Vaucouleurs et al. 1991, hereafter RC3) as the galaxy is nearly round.

NGC 2681 FIRST lists a peak 20 cm flux density of 3.8 mJy/beam at 5'' resolution, with extended emission in P.A. 35°. We did not detect this object at 2 cm. The UGC and RC3 do not list a P.A. for this galaxy as it is almost round.

NGC 2787 Heckman et al. (1980) find 20 cm and 6 cm peak flux-densities of <9 mJy/beam and 9 mJy/beam, at resolutions of 4'' and 1''.7, respectively, so the nucleus has a flat or inverted spectrum between 20 cm and 6 cm, $\alpha_6^{20} \geq 0$. Combining the 6 cm peak flux-density with our 2 cm peak flux-densities of 7 mJy/beam and 8.9 mJy/beam at resolutions of 0''.15 and 5'', respectively, results in a non-simultaneous spectral index, α_2^6 between -0.2 and 0 , for all emission within the central 1''.7.

NGC 3147 Vila et al. (1990) find $S_{20cm}^{peak} = 10.6$ mJy/beam and $S_{6cm}^{peak} = 8.55$ mJy/beam at resolutions of $\sim 1''.2$ and $\sim 1''.5$, respectively, with both maps showing only a compact core. Consistent with this, Laurent-Muehleisen et al. (1997) find a nuclear peak flux-density of 9 mJy/beam at 6 cm at a resolution of 0''.4. Combining this 6 cm flux density with our 2 cm peak flux-density (8 mJy/beam), the non-simultaneous spectral index of the emission in the central 0''.4 is flat, $\alpha_2^6 \geq 0$.

NGC 3169 Hummel et al. (1987) find a core flux-density of 8.2 mJy in the central 2'' of their 1''.2 resolution, 20 cm map, and also extended emission in P.A. 120°, more or less along the minor axis of the host galaxy. Combining their 20 cm peak flux-density with our measured 2 cm peak flux-densities of 6.8 mJy/beam and 10 mJy/beam at resolutions of 0''.15 and 5'', respectively, results in a non-simultaneous spectral index, α_2^{20} , between -0.1 and 0.1 , for the radio emission within the central 2''.

NGC 4111 FIRST lists this object's peak 20 cm flux density as 5.8 mJy/beam at 5'' resolution. The emission is extended in P.A. 70°, along the minor axis of the host galaxy. We did not detect this object at 2 cm.

NGC 4143 - Wrobel & Heeschen (1991) find a 6 cm flux density of 6.7 mJy at 5'' resolution. The similar resolution (5'') FIRST map shows a peak flux-density of 5 mJy/beam at 20 cm, with extended emission in P.A. 10°, which is not along the minor axis of the host galaxy. Combining the FIRST peak flux-density with our 2 cm peak flux-densities of 3.3 mJy/beam and 5.3 mJy/beam at resolutions of 0''.15 and 5'', respectively, results in a non-simultaneous spectral index, α_2^{20} between -0.2 and 0 , for all emission within the central 5''. Ho et al. (1997b) note that broad H β may also be present in this object.

NGC 4203 Wrobel (1991) derived a 6 cm flux density of 12.5 mJy at $\sim 5''$ resolution, and FIRST lists a peak 20 cm flux density of 6.9 mJy/beam (at a resolution of 5''), implying that the core has

a highly inverted spectrum between 20 cm and 6 cm, $\alpha_6^{20} \sim 0.5$. Our D-configuration 2 cm flux density of 12.3 mJy, suggests a non-simultaneous spectral index $\alpha_2^6 \sim 0$. The extended emission in the FIRST map is in P.A. 90° , more or less along the minor axis of the host galaxy.

NGC 4216 Hummel et al. (1987) observed this object with $1''.3$ resolution at 20 cm and did not detect any emission in the central $2''$ of the galaxy, at a 3σ upper limit of 0.5 mJy.

NGC 4278 Jones (1984) have observed this object using VLBI and find the core flux density is 180 mJy and 190 mJy at 18 cm and 6 cm, on size scales <5 mas and <1 mas, respectively. Wilkinson et al. (1998) find a 3.6 cm peak flux-density of 153 mJy/beam at 200 mas resolution, and we find a 2 cm peak flux-density of 88.3 mJy/beam at 150 mas resolution, so the core may be flat between 18 and 6 cm and then steeper down to 2 cm. Alternatively, the lower flux density at 2 cm may be due to source variability. The 20 cm emission detected in FIRST is extended in P.A. 166° , but the UGC and RC3 do not list a host galaxy P.A. as the galaxy is almost round.

NGC 4419 Hummel et al. (1987) find a core flux-density of 32 mJy in the central $2''$ of their $1''.3$ resolution 20 cm map, and extended emission in P.A. 77° . Combining this flux density with our 2 cm D-configuration peak flux-density of 5.4 mJy/beam at $5''$ resolution, results in a non-simultaneous spectral index, $\alpha_2^{20} \leq -0.8$. This object was not detected in our $0''.15$ resolution, 2 cm A-configuration map.

NGC 4449 FIRST lists a 20 cm peak flux-density of 1.7 mJy/beam at $5''$ resolution, with extended emission in P.A. 65° , more or less along the host galaxy major axis. We did not detect this object at 2 cm.

NGC 4527 Vila et al. (1990) find $S_{20cm}^{peak} = 4.3$ mJy/beam and $S_{6cm}^{peak} = 1.3$ mJy/beam at resolutions of $\sim 1''.3$ and $\sim 1''.4$, respectively (a spectral index, α_6^{20} , of about -1.1). The 20 cm and 6 cm maps are both highly extended (P.A. 65°) along the major axis of the galaxy, with an edge brightened morphology, suggestive of an annulus (Vila et al. 1990). We did not detect this galaxy at 2 cm.

NGC 4548 Hummel et al. (1987) find a 3σ upper limit of 2.5 mJy at 20 cm, over the central $2''$ of their $1''.3$ resolution VLA map. Since we detect a flux density of 1.2 mJy at 2 cm, the non-simultaneous spectral index of the core is $\alpha_2^{20} \geq -0.3$.

NGC 4550 The 2 cm source we detect is offset $9''.3$ west and $5''.5$ north of the optical position determined by Cotton et al. (1999) from digital sky survey plates. The 1σ error of the optical

position determination is estimated to be $2''.3$ in each of the R.A. and Dec. The galaxy does not show any obvious sign of a peculiar morphology, and the east-west galaxy extent is $\sim 1'$, so the radio-optical offset does appear significant. A $\sim 3''$ resolution 11 cm map (Haynes & Sramek 1980) shows an unresolved radio core at a position between our radio detection and the optical nucleus. Wrobel & Heeschen (1991) find the 6 cm emission over the central $5''$ is < 1 mJy. We measure a 2 cm peak flux-density of 0.7 mJy/beam, so the source is probably flat spectrum, $\alpha_2^6 \geq -0.3$.

NGC 4565 Hummel et al. (1987) find a core 20 cm flux density of 1.2 mJy in the central $2''$ of their $1''.3$ resolution VLA map. FIRST lists a peak flux-density of 1.5 mJy/beam at 20 cm in a $5''$ resolution map, with extended emission in P.A. 36° , along the minor axis of the host galaxy. Combined with our 2 cm peak flux-density of 3.7 mJy/beam at $0''.15$ resolution, the non-simultaneous spectral index is $\alpha_2^{20} \geq 0.5$. This galaxy has the lowest broad H α luminosity found in any known active nucleus (Ho et al. 1997b).

NGC 4579 Hummel et al. (1987) find a core flux-density of 25.1 mJy in the central $2''$ of their $1''.3$ resolution, 20 cm VLA map, with extended emission in P.A. $\sim 135^\circ$. The radio core was found to have an inverted spectrum between 13 cm and 3.6 cm with the Parkes-Tidbinbilla 275 km interferometer ($S_\nu \propto \nu^{0.2}$; Sadler et al. 1995). Van der Hulst, Crane & Keel (1981) found the 6 cm emission to be extended in P.A. 134° , with extent $0''.4 \pm 0''.2$ and flux density 39.9 mJy.

NGC 4636 We derive a peak 2 cm flux density of 1.6 mJy/beam for this galaxy. Stanger & Warwick (1986) have imaged this object at $4''$ resolution at 6 cm and 20 cm. Both maps show extended jet-like structure in P.A. $\sim 45^\circ$, more or less along the minor axis of the host galaxy. They found a peak 20 cm flux density of 11.4 mJy/beam, and a steep spectrum ($\alpha = -0.6$) over the jets and at the core. The steep-spectrum jets may dominate the core emission within the central $4''$ beam, so the core could potentially have a flat spectrum at higher resolution. In the absence of higher resolution maps, we list this object as a steep spectrum source in Table 1.

NGC 5005 Vila et al. (1990) find $S_{20cm}^{peak} = 14.6$ mJy/beam and $S_{6cm}^{peak} = 2.7$ mJy/beam at resolutions of $\sim 1''.1$ and $\sim 1''.0$, respectively (a spectral index of $\alpha_6^{20} = -1.8$). The source is resolved at both wavelengths, in P.A. $\sim 135^\circ$ on a $\sim 5''$ scale, again more or less along the minor axis of the host galaxy. Hummel et al. (1985) find a 20 cm peak flux-density of 70 mJy/beam at $14''$ resolution, with extended emission (about $2'$ extent) in P.A. 67° , along the major axis of the galaxy. FIRST also lists this source with a peak 20 cm flux density of 35.9 mJy/beam (at $5''$ resolution), with extended emission in P.A. 124° . The relatively steep spectral slope between 20 and 6 cm, and the extended radio morphology at these frequencies, is consistent with our 2 cm non-detection.

NGC 5033 FIRST lists a peak flux-density of 1.4 mJy/beam at 20 cm at a resolution of 5". The inner radio emission in the FIRST map is extended in P.A. 91°, along the minor axis of the host galaxy, and there is an outer diffuse component which is more aligned with the host galaxy major axis. Combining the FIRST peak flux-density with our 2 cm peak flux-density (1.4 mJy/beam) results in a non-simultaneous spectral index $\alpha_2^{20} \geq 0$.

NGC 5055 The 20 cm FIRST map has peak flux-density 1.5 mJy/beam, and shows extended emission in P.A. 42°. We did not detect this galaxy at 2 cm.

NGC 5273 FIRST lists a peak flux-density of 2.6 mJy/beam at 20 cm; the extended radio emission (P.A. 180°) is along the major axis of the host galaxy disk. We did not detect this galaxy at 2 cm.

NGC 5866 Condon et al. (1990) find a peak 20 cm flux density of 9.5 mJy/beam in a 5" resolution map made with the VLA. This is somewhat different from the value listed in FIRST - 20 cm peak flux-density of 15.4 mJy/beam at a resolution of 5". Wrobel & Heeschen (1991) derived a flux density of 7.4 mJy from their 5" resolution 6 cm map. We measured a peak 2 cm flux density of 7.1 mJy/beam at 0".15 resolution, so the core has a spectral index, $\alpha_2^6 \geq 0$. The extended flux density in the FIRST map is in P.A. 132°, along the major axis of the host galaxy, not unexpected in this transition object. This is the only transition object in the sample in which we detected a 2 cm radio core.

NGC 6500 The spectrum of the core of this spiral is known to be flat on scales of ~ 20 mas (Jones et al. 1981). The 1".2 resolution 20 cm map of Unger et al. (1989) shows extended emission in P.A. 140°, along the minor axis of the galaxy, suggestive of an outflow. Their higher resolution (0".3) 20 cm MERLIN map shows an extension in P.A. $\sim 70^\circ$.

NGC 7217 Our simultaneous 3.6 cm observation on 1996 October 11, with resolution 0".27 x 0".25, detected an unresolved nuclear source with flux density 1.2 mJy. Since the 3.6 cm detection gives us an accurate position for the radio core, we use a 5σ upper limit of 0.6 mJy at 2 cm.

REFERENCES

- Alonso-Herrero, A., Rieke, M. J., Rieke, G. H., & Shields, J. C. 2000, ApJ, 530, 688
Baars, J. W. M., Genzel, R., Pauliny-Toth, I. I. K., & Witzel, A. 1977, A&A, 61, 99
Bartel, N., et al. 1982, ApJ, 262, 556

- Barth, A. J., Filippenko, A. V., Moran, E. C. 1999, *ApJ*, 525, 673
- Barth, A. J., Ho, L. C., Filippenko, A. V., & Sargent, W. L. W. 1998, *ApJ*, 496, 133
- Barth, A. J., Reichert, G. A., Filippenko, A. V., Ho, L. C., Shields, J. C., Mushotzky, R. F., & Puchnarewicz, E. M. 1996, *AJ*, 112, 1829
- Baum, S. A., & Heckman, T. M. 1989, *ApJ*, 336, 702
- Begelman, M. C., Blandford, R. D., & Rees, M. J. 1984, *Rev. Mod. Phys.*, 56, 255
- Blandford, R. D. 1993, in *Astrophysical Jets*, ed. D. Burgarella, M. Livio, & C. P. O’Dea, (Cambridge: Cambridge Univ. Press), 15
- Braatz, J., Wilson, A. S., & Henkel, C. 1997, *ApJS*, 110, 321
- Clarke, C. J., Kinney, A. L., & Pringle, J. E. 1998, *ApJ*, 495, 189
- Colbert, E. J., Baum, S. A., Gallimore, J. F., O’Dea, C. P., & Christensen, J. A. 1996, *ApJ*, 467, 551
- Condon, J. J., Helou, G., Sanders, D. B., & Soifer, B. T. 1990, *ApJS*, 73, 359
- Condon, J. J., Huang, Z.-P., Yin, Q. F., & Thuan, T. X. 1991 *ApJ*, 378, 65
- Cotton, W. D., Condon, J. J., & Arbizani, E. 1999, *ApJS*, 125, 409
- de Bruyn, A. G., & Wilson, A. S. 1978, *A&A*, 64, 433
- de Vaucouleurs, G., de Vaucouleurs, A., Corwin, H. G., Buta, R. J., Paturel, G., & Fouqué, P. 1991, *Third Reference Catalogue of Bright Galaxies* (New York: Springer-Verlag) (RC3)
- Dopita, M. A., & Sutherland, R. S. 1995, *ApJ*, 455, 468
- Falcke, H. 1996, *ApJ*, 464, L67
- Falcke, H. & Biermann, P. L. 1996, *A&A*, 308, 321
- Falcke, H. & Biermann, P. L. 1999, *A&A*, 342, 49
- Falcke, H., Ho, L. C., Ulvestad, J., Wilson, A. S., & Nagar, N. M. 1998, in *Proceedings of the International Symposium on Astr. Research and Sci. education at the Vatican Observatory*, ed. C. Impey
- Falcke, H., Nagar, N. M., Wilson, A. S., Ho, L. C., & Ulvestad, J. S. 2000, in *Black Holes in Binaries and Galactic Nuclei*, ed. L. Kaper, E. P. J. van den Heuvel, & P. A. Woudt, (Berlin: Springer), in press
- Falcke, H., Nagar, N. M., Wilson, A. S., & Ulvestad, J. S. 2000, *ApJ*, submitted (Paper II)

- Falcke, H., Wilson, A. S., & Ho, L. C. 1997, in *Relativistic Jets in AGNs*, Proceedings of the International Conference, ed. M. Ostrowski, M. Sikora, G. Madejski, & M. Begelman, (Kraków), 13
- Filippenko, A. V., & Terlevich, R. 1992, *ApJ*, 397, L79
- Fosbury, R. A. E., Mebold, U., Goss, W. M., & Dopita, M. A. 1978, *MNRAS*, 183, 549
- Gallimore, J. F., Baum, S. A., O’Dea, C. P., Pedlar, A., & Brinks, E. 1999, *ApJ*, 524, 684
- Graham, D. A., Weiler, K. W., & Wielebinski, R. 1981, *A&A*, 97, 388
- Haynes, M., & Sramek, R. 1980, *AJ*, 80, 673
- Heckman, T. M. 1980, *A&A*, 87, 152
- Heckman, T. M., Balick, B., & Crane, P. C. 1980, *A&AS*, 40, 295
- Helou, G., Madore, B. F., Schmitz, M., Bica, M. D., Wu, X., & Bennett, J. 1991, in *Databases and On-Line Data in Astronomy*, ed. D. Egret & M. Albrecht (Dordrecht: Kluwer), 89
- Ho, L. C. 1999, *ApJ*, 516, 672
- Ho, L. C., et al. 2000, in preparation
- Ho, L. C., Filippenko, A. V., & Sargent, W. L. W. 1993, *ApJ*, 417, 63
- Ho, L. C., Filippenko, A. V., & Sargent, W. L. W. 1995, *ApJS*, 98, 477
- Ho, L. C., Filippenko, A. V., & Sargent, W. L. W. 1997a, *ApJS*, 112, 315 (H97a)
- Ho, L. C., Filippenko, A. V., & Sargent, W. L. W., & Peng, C. Y. 1997b, *ApJS*, 112, 391
- Hummel, E. 1980, *A&AS*, 41, 151
- Hummel, E., Pedlar, A., van der Hulst, J. M., & Davies, R. D. 1985, *A&AS*, 60, 293
- Hummel, E., van der Hulst, J. M., Keel, W. C., & Kennicutt, R. C. 1987, *A&AS*, 70, 517
- Jones, D. L. 1984, *ApJ*, 287, 33
- Jones D. L., Sramek R. A., & Terzian Y. 1981, *ApJ*, 246, 28
- Keel, W. C., & Hummel, E. 1988, *A&A*, 194, 90
- Koski, A. T., & Osterbrock, D. E. 1976, *ApJ*, 203, L49
- Laurent-Muehleisen, S. A., Kollgaard, R. I., Ryan, P. J., Feigelson, E. D., Brinkmann, W., & Siebert, J. 1997, *A&AS*, 122, 235

- Lavalley, M., Isobe, T., & Feigelson, E. 1992, in *Astronomical Data Analysis Software and Systems I*, ed. Worrall, D., Biemesderfer, C., & Barnes, J., (San Francisco: ASP), Vol. 25, 245 (ASURV)
- Lovelace, R. V. E., & Romanova, M. M. 1996, in *Energy Transport in Radio Galaxies*, ed. P. E. Hardee, A. H. Bridle, & J. A. Zensus (San Francisco: ASP), Vol. 100, 25
- Lynden-Bell, D., & Rees, M. J. 1971, *MNRAS*, 152, 461
- Magorrian, J., et al. 1998, *AJ*, 115, 2285
- Maoz, D., Filippenko, A. V., Ho, L. C., Rix, H.-W., Bahcall, J. N., Schneider, D. P., & Macchetto, F. D. 1995, *ApJ*, 440, 91
- Maoz, D., Koratkar, A. P., Shields, J. C., Ho, L. C., Filippenko, A. V., & Sternberg, A. 1998, *AJ*, 116, 55
- Melia, F. 1992, *ApJ*, 398, L95
- Melia, F. 1994, *ApJ*, 426, 577
- Nagar, N. M., Wilson, A. S., Mulchaey, J. S., & Gallimore, J. F. 1999a, *ApJS*, 120, 209
- Nagar N. M., Falcke, H., Wilson, A. S., & Ho, L. C. 1999b, in *Lifecycles of Radio Galaxies*, ed. J. Biretta et al., *New Astronomy Reviews*, in press
- Nagar, N. M., & Wilson, A. S. 1999, *ApJ*, 516, 97
- Nagar, N. M., et al. 2000, in preparation (Paper IV)
- Napier, P. J., Bagri, D. S., Clark, B. G., Rogers, A. E. E., Romney, J. D., Thompson, A. R., & Walker, R. C. 1994, *Proc. IEEE*, 82, 658
- Narayan, R., Mahadevan, R., & Quataert, E. 1998, in *The Theory of Black Hole Accretion Discs*, ed. M. A. Abramowicz, G. Björnsson, & J. E. Pringle (Cambridge: Cambridge Univ. Press), 148
- Nilson, P. 1973, *Uppsala General Catalogue of Galaxies* (Royal Society of Sciences of Uppsala) (UGC)
- Osterbrock, D. E. 1981, *ApJ*, 249, 462
- Peng, C. Y., Ho, L. C., Filippenko, A. V., & Sargent, W. L. W. 1999, *BAAS*, 193, 0607
- Pringle, J. E. 1993, in *Astrophysical Jets*, ed. D. Burgerella, M. Livio, & C. P. O’Dea, (Cambridge: Cambridge Univ. Press), 1
- Pringle, J. E. 1997, *MNRAS*, 292, 136

- Ptak, A., Yaqoob, T., Mushotzky, R., Serlemitsos, P., & Griffiths, R. 1998, *ApJ*, 501, L37
- Quataert, E., Di Matteo, T., Narayan, R., & Ho, L. C. 1999, *ApJ*, 525, L89
- Rees, M. J., Begelman, M. C., Blandford, R. P., & Phinney, E. S. 1982, *Nature*, 295, 17
- Richstone, D., et al. 1998, *Nature*, 395A, 14
- Sadler, E. M., Jenkins, C. R., & Kotanyi, C. G. 1989, *MNRAS*, 240, 591
- Sadler, E. M., Slee, O. B., Reynolds, J. E., & Roy, A. L. 1995, *MNRAS*, 276, 1373
- Shields, J. C. 1992, *ApJ*, 399, L27
- Shields, J. C., et al. 2000, *ApJ*, in press (astro-ph/0004047)
- Smith, H. E., Lonsdale, C. J., & Lonsdale, C. J. 1998, *ApJ*, 492, 137
- Schmitt, H. R., Kinney, A. L., Storchi-Bergmann, T., & Antonucci, R. 1997, *ApJ*, 477, 623, and
Erratum *ApJ*, 485, 434
- Slee, O. B., Sadler, E. M., Reynolds, J. E., & Ekers, R. D. 1994, *MNRAS*, 269, 928
- Stanger, V. J., & Warwick, R. S. 1986, *MNRAS*, 220, 363
- Terashima, Y., Ho, L. C., Ptak, A. F., Mushotzky, R. F., Serlemitsos, P. J., Yaqoob, T., & Kunieda, H. 2000, *ApJ*, in press (astro-ph/9911340)
- Terashima, Y., Kunieda, H., Misaki, K., Mushotzky, R. F., Ptak, A. F., & Reichert, G. A. 1998, *ApJ*, 503, 212
- Terashima, Y., Yaqoob, T., Serlemitsos, P. J., Kunieda, H., Misaki, K., Ptak, A. F., & Ho, L. C. 2000, *ApJ*, submitted
- Terlevich, R., & Melnick J. 1985, *MNRAS*, 213, 841
- Terlevich, R., Tenorio-Tagle, G., Franco, J., & Melnick, J. 1995, *MNRAS*, 272, 198
- Thompson, A. R., Clark, B. G., Wade C. M., & Napier, P. J. 1980, *ApJS*, 44, 151
- Ulvestad, J. S., & Wilson, A. S. 1984, *ApJ*, 285, 439
- Ulvestad, J. S., & Wilson, A. S. 1989, *ApJ*, 343, 659
- Ulvestad, J. S., Wilson, A. S., & Sramek, R. A. 1981, *ApJ*, 247, 419
- Unger, S. W., Pedlar, A., & Hummel, E. 1989, *A&A*, 208, 14
- van der Hulst, J. M., Crane, P. C., & Keel, W. C. 1981, *AJ*, 86, 1175

Vila, M. B., Pedlar, A., Davies, R. D., Hummel, E. & Axon, D. J. 1990, MNRAS, 242, 379

White, R. L., Becker, R. H., Helfand, D. J., & Gregg, M. D. 1997, ApJ, 475, 479 (FIRST)

Wilkinson, P. N., Browne, I. W. A., Patnaik, A. R., Wrobel, J. M., & Sorathia, B. 1998, MNRAS, 300, 790

Wrobel, J. M. 1991, AJ, 101, 127

Wrobel, J. M., & Heeschen, D. S. 1991, AJ, 101, 148

Zensus, A. 1997, ARA&A, 35, 607

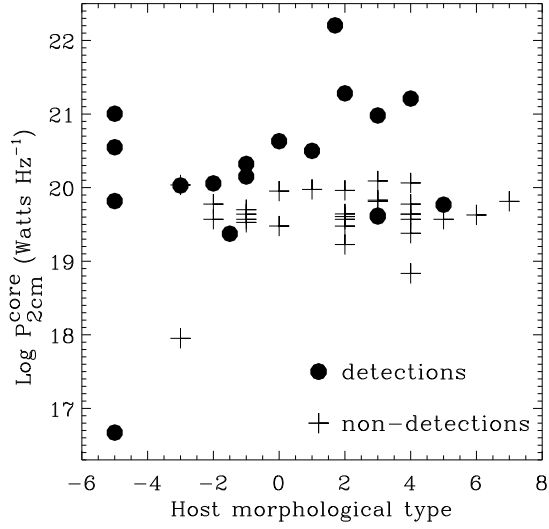


Fig. 1.— Distribution of the 2 cm nuclear power for all 48 LLAGNs in the sample, as a function of host galaxy morphological type. Detections are plotted with filled circles while non-detections are plotted with crosses. Note the large number of spiral galaxies detected.

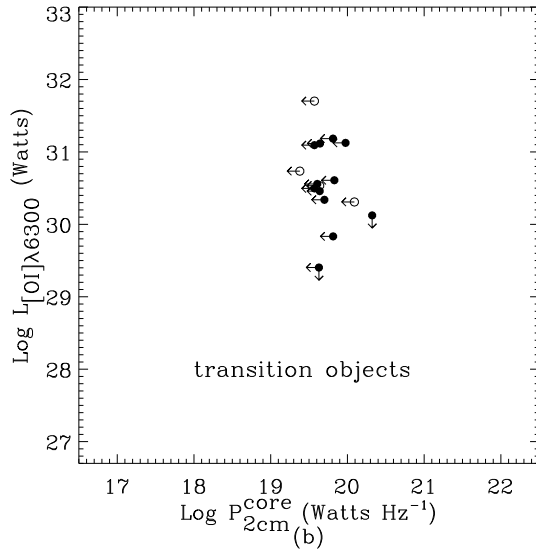
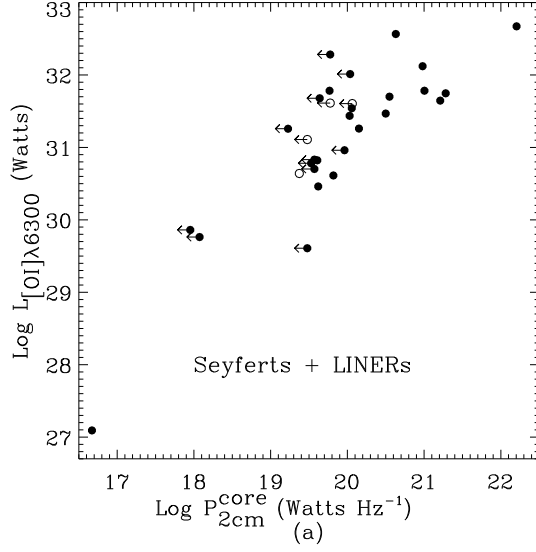


Fig. 2.— (a) Relationship between $[O\ I] \lambda 6300\text{\AA}$ luminosity and 2 cm radio power for Seyfert and LINER nuclei in our sample. Objects with non-photometric $[O\ I] \lambda 6300\text{\AA}$ flux measurements are shown as open circles; (b) same as (a) but for transition nuclei in our sample.

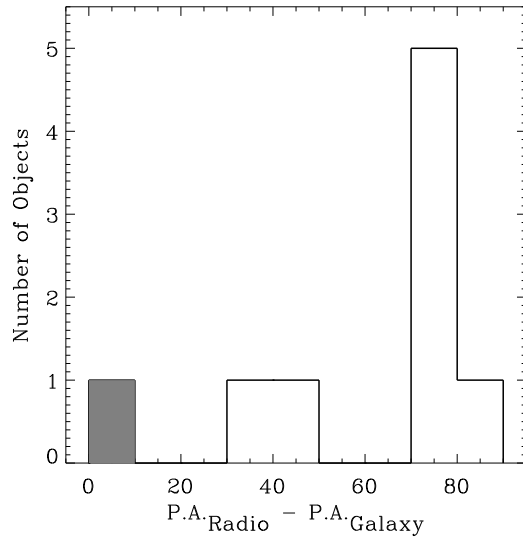


Fig. 3.— Histogram of the distribution of the difference between the position angle of the 20 cm radio emission at $1''$ – $5''$ resolution and the position angle of the host galaxy major axis, as listed in the UGC, for all LLAGNs in our sample which contain a 2 cm compact core and have extended nuclear radio emission. The single transition object is shown in grey.

TABLE 1
NEW 2 CM VLA OBSERVATIONS OF LOW-LUMINOSITY AGNs

Name	Activity Type	T	R.A. (B1950)	Dec. (B1950)	Δ ($''$)	Peak A (mJy/ beam)	Total A (mJy)	Peak D (mJy/ beam)	Total D (mJy)	Dist. (Mpc)	Log P_{2cm}^{core} ($W Hz^{-1}$)	α	Com.
(1)	(2)	(3)	(4)	(5)	(6)	(7)	(8)	(9)	(10)	(11)	(12)	(13)	(14)
NGC 185	S2	-5.0	00 36 09.993	48 03 50.20	14.5	0.8	0.8	0.7	16.67	?	2,6
NGC 266	L1.9	2.0	00 47 05.247	32 00 20.04	1.9	4.1	4.1	62.4	21.28	F	2,4
NGC 404	L2	-3.0	< 1.3	< 1.3	2.4	< 17.95	...	2,4
NGC 2655	S2	0.0	08 49 08.450	78 24 48.31	2.4	6.0	6.0	13.4	13.6	24.4	20.63	S	1
NGC 2681	L1.9	0.0	< 1.4	< 1.4	< 1.4	< 1.4	13.3	< 19.48	...	1
NGC 2787	L1.9	-1.0	09 14 49.468	69 24 50.81	1.6	7.0	7.0	8.9	9.0	13.0	20.15	F	1
NGC 3147	S2	4.0	10 12 39.818	73 39 00.79	1.6	8.0	8.1	10.2	10.3	40.9	21.21	F	1
NGC 3169	L2	1.0	10 11 39.413	03 42 52.60	3.5	6.8	6.8	10.0	10.7	19.7	20.50	F	1
NGC 3226	L1.9	-5.0	10 20 43.173	20 09 06.52	0.9	5.0	5.4	5.6	5.9	23.4	20.55	F	1
NGC 3642	L1.9	4.0	< 1.3	< 1.3	< 1.3	< 1.3	27.5	< 20.06	...	1
NGC 3692	T2	3.0	< 1.2	< 1.2	< 1.2	< 1.2	29.8	< 20.09	...	1
NGC 3705	T2	2.0	< 1.2	< 1.2	< 1.2	< 1.2	17.0	< 19.61	...	1
NGC 3917	T2:	6.0	< 1.2	< 1.2	< 1.2	< 1.2	17.0	< 19.63	...	1
NGC 3953	T2	4.0	< 1.3	< 1.3	< 1.3	< 1.3	17.0	< 19.64	...	1
NGC 3992	T2:	4.0	< 1.3	< 1.3	< 1.3	< 1.3	17.0	< 19.64	...	1
NGC 4036	L1.9	-3.0	11 58 52.765	62 10 27.73	2.4	< 1.5	< 1.5	1.5	1.5	24.6	< 20.04	...	1
NGC 4111	L2	-1.0	< 1.3	< 1.3	< 1.3	< 1.3	17.0	< 19.64	...	1
NGC 4143	L1.9	-2.0	12 07 04.547	42 48 44.27	1.5	3.3	3.3	5.3	5.5	17.0	20.06	F	1
NGC 4145	T2:	7.0	< 1.3	< 1.3	< 1.3	< 1.3	20.7	< 19.81	...	1
NGC 4192	T2	2.0	12 11 15.488	15 10 39.62	1.5	< 1.3	< 1.3	1.3	1.3	16.8	< 19.64	...	1
NGC 4203	L1.9	-3.0	12 12 33.943	33 28 30.35	1.0	9.5	9.5	12.3	13.3	9.7	20.03	F	1
NGC 4216	T2	3.0	12 13 21.559	13 25 38.16	0.5	< 2.0	< 2.0	2.0	2.0	16.8	< 19.83	...	1
NGC 4220	T2	-1.0	< 1.4	< 1.4	< 1.4	< 1.4	17.0	< 19.70	...	1
NGC 4278	L1.9	-5.0	12 17 36.158	29 33 29.29	1.5	88.3	89.7	95.9	96.5	9.7	21.00	F	1
NGC 4419	T2	1.0	12 24 24.661	15 19 25.84	3.2	< 2.8	< 2.8	5.4	7.4	16.8	< 19.98	...	1
NGC 4429	T2	-1.0	< 1.1	< 1.1	16.8	< 19.57	...	3
NGC 4435	T2/H:	-2.0	< 1.1	< 1.1	16.8	< 19.57	...	3
NGC 4527	T2	4.0	< 1.1	< 1.1	13.5	< 19.38	...	3
NGC 4548	L2	3.0	12 32 55.276	14 46 17.60	1.8	1.2	1.2	16.8	19.61	F	3
NGC 4550	L2	-1.5	12 32 58.493	12 29 49.50	9.3	0.7	0.7	16.8	19.37	F	3,6
NGC 4565	S1.9	3.0	12 33 52.014	26 15 45.87	3.9	3.7	3.7	9.7	19.62	F	3
NGC 4569	T2	2.0	< 1.1	< 1.1	16.8	< 19.57	...	3
NGC 4579	S1.9/L1.9	3.0	12 35 12.000	12 05 34.85	0.7	27.6	28.3	16.8	20.98	F	3
NGC 4636	L1.9	-5.0	12 40 16.660	02 57 41.64	2.5	1.6	1.9	17.0	19.82	S	3
NGC 4639	S1.0	4.0	< 1.1	< 1.1	16.8	< 19.57	...	3
NGC 4651	L2	5.0	< 1.1	< 1.1	16.8	< 19.57	...	3
NGC 4866	L2	-1.0	< 1.1	< 1.1	16.0	< 19.53	...	3
NGC 5005	L1.9	4.0	< 1.1	< 1.1	21.3	< 19.78	...	3
NGC 5033	S1.5	5.0	13 11 09.169	36 51 30.37	1.3	1.4	1.4	18.7	19.77	F	3
NGC 5055	T2	4.0	< 1.1	< 1.1	7.2	< 18.83	...	3
NGC 5273	S1.5	-2.0	< 1.1	< 1.1	21.3	< 19.78	...	3
NGC 5566	L2	2.0	< 1.1	< 1.1	26.4	< 19.96	...	3
NGC 5701	T2:	0.0	< 1.1	< 1.1	26.1	< 19.95	...	3
NGC 5866	T2	-1.0	15 05 07.121	55 57 17.77	0.3	7.1	7.5	15.3	20.32	F	3
NGC 6500	L2	1.7	17 53 48.137	18 20 39.90	1.5	83.5	85.0	39.7	22.21	F	3
NGC 7217	L2	2.0	22 05 37.830	31 06 51.50	2.7	< 0.6	< 0.6	16.0	< 19.23	...	2,4,5
NGC 7742	T2/L2	3.0	< 1.1	< 1.1	22.2	< 19.81	...	2
NGC 7814	L2::	2.0	< 1.1	< 1.1	15.1	< 19.48	...	2

Columns are: (1) galaxy name; (2) nuclear activity type as given by H97a. ‘L’ represents LINER, ‘S’ represents Seyfert, ‘H’ represents an H II region type spectrum, and ‘T’ represents objects with transitional ‘L’ + ‘H’ spectra. ‘2’ implies that no broad H α is detected, ‘1.9’ implies that broad H α is present, but not broad H β , and ‘1.0’ or ‘1.5’ implies that both broad H α and broad H β are detected, with the specific type depending on the ratio of the flux in [O III] λ 5007 to the flux in broad + narrow H β (e.g. Osterbrock 1981). The ‘:’ and ‘::’ symbols represent uncertain, and highly uncertain, classifications, respectively; (3) Hubble morphological parameter T as listed in H97a; (4) and (5) 2 cm radio position, from our maps; (6) offset, in arcsec, between the 2 cm radio position and the position of the galaxy optical nucleus listed in Cotton et al. 1999; (7) and (8) peak and total flux-density, obtained by fitting a single Gaussian (with peak flux-density, major and minor axes as free parameters) to the nuclear radio source in the A-configuration image; (9) and (10) similar to (7) and (8), but for the D-configuration image, when available; (11) distance in Mpc to galaxy, as listed in H97a; (12) the logarithm of the core radio power (derived from the *peak* radio flux in the A-configuration image); (13) indication of whether the radio spectrum of the A-configuration 2 cm detected core is *Steep* ($\alpha < -0.3$; $S_\nu \propto \nu^\alpha$), or *Flat* ($\alpha \geq -0.3$); see Appendix A; (14) Comments as listed below.

Notes: NGC 5756 (not part of the Palomar spectroscopic sample), and NGC 4449 (which has a H II region-type nuclear spectrum) were also observed, but not detected at a 10σ limit of 1.1 mJy.

Comments: (1) October 7 run; (2) October 11 run; (3) October 18 run; (4) also observed at 0.7 cm and 3.6 cm, see Section 2 and Appendix A; (5) radio position is from the 3.6 cm detection. For this object a 5σ upper limit is used at 2 cm, see Appendix A; (6) possibly not the position of the nucleus, see Sec 3.1 and Appendix A.

TABLE 2
RADIO AND HOST GALAXY POSITION ANGLES

Name	Activity type	20 cm Radio P.A.	Host Galaxy Major Axis P.A.
NGC 3169	L2	120	45
NGC 4143	L1.9	10	144
NGC 4203	L1.9	89	10
NGC 4565	S1.9	36	136
NGC 4579	S1.9/L1.9	134	95
NGC 4636	L1.9	45	150
NGC 5033	S1.5	91	170
NGC 5866	T2	132	128
NGC 6500	L2	140	50

Columns are: (1) galaxy name; (2) activity type, as listed in Table 1, column 2; (3) position angle of the radio emission measured from the 20 cm FIRST image (5'' resolution) or other 20 cm image at 1''–5'' resolution (see Appendix A for details); (4) position angle of the host galaxy major axis as listed in UGC. Position angles are measured North through East, and are in degrees.